

General Self-Template Synthesis of Transition-Metal Oxide and Chalcogenide Mesoporous Nanotubes with Enhanced Electrochemical Performances

Huan Wang⁺, Sifei Zhuo⁺, Yu Liang, Xiling Han, and Bin Zhang*

Abstract: The development of a general strategy for synthesizing hierarchical porous transition-metal oxide and chalcogenide mesoporous nanotubes, is still highly challenging. Herein we present a facile self-template strategy to synthesize Co_3O_4 mesoporous nanotubes with outstanding performances in both the electrocatalytic oxygen-evolution reaction (OER) and Li-ion battery via the thermal-oxidation-induced transformation of cheap and easily-prepared Co-Asp (cobalt-aspartic acid) nanowires. The initially formed thin layers on the precursor surfaces, oxygen-induced outward diffusion of interior precursors, the gas release of organic oxidation, and subsequent Kirkendall effect are important for the appearance of the mesoporous nanotubes. This self-template strategy of low-cost precursors is found to be a versatile method to prepare other functional mesoporous nanotubes of transition-metal oxides and chalcogenides, such as NiO , NiCo_2O_4 , Mn_3O_8 , CoS_2 and CoSe_2 .

Hollow and porous nanostructures of semiconductors have achieved various promising applications as a result of their unique structure-dependent physical/chemical properties.^[1] Especially, the unique anisotropic geometry of nanotubes is driving the exploration of synthetic strategies to rationally design hierarchical porous nanotubes with open-ended channels and mesoporous walls.^[2] The convenient permeation of electrolyte, the short transport distance of electrons as well as the enhanced active sites guarantee the excellent performance of hierarchical porous nanotubes in a variety of fields including catalysis, energy storage, and sensors. Simultaneously, self-template directed strategy derived from chalcogenides,^[3] hydroxides,^[4] organic-inorganic hybrids,^[5] and metal-organic frameworks (MOFs)^[6], has been regarded as an effective method for the fabrication of hollow nanostructures. For instance, a wide variety of multishelled and multicompositional hollow nanostructures have been systematically reported by the Lou group and the Wang group.^[7] Zhang et al. also achieved hierarchical nanotubes and hollow nano-

sheets via an ion-exchange route of inorganic-organic nanohybrids.^[4a,5] However, the proposed methods are always restricted to spheres or specific compounds due to the deficiency of universal, cheap, sacrificial templates, and the as-prepared products always have closed morphology rather than open-ended structures. Therefore, the exploration of versatile sacrificial templates for the chemical transformation synthesis of a sequence of porous nanotubes, especially with open tubular structure, is highly desirable.

Transition-metal oxides (TMOs) and chalcogenides (TMCs) have been recognized as significant materials due to their promising applications in many fields.^[8] Among them, cobalt-based TMOs and TMCs (e.g. Co_3O_4 , NiCo_2O_4 , CoS_2 , and CoSe_2) are attracting increasing attention because of their good performance in photo- and electrochemical reductions,^[9] Li-ion batteries,^[10] oxygen-evolution reaction (OER),^[11] hydrogen-evolution reaction (HER),^[12] and magnetic properties^[13] have been achieved. Thus, great effort has been devoted to the controlled synthesis of TMOs and TMCs. Although great advances have been made on the synthesis of nanotubes, -wires, -particles, and -cages, the development of a universal method to synthesize hierarchical porous cobalt-based TMOs and TMCs with mesoporous walls and open-ended tubes is still a great challenge.

Herein, we demonstrate a self-template strategy to synthesize hierarchical porous nanotubes of Co_3O_4 via the oxidation-induced transformation of cobalt-Asp (aspartic acid, a simple, cheap, and commercially available amino acid) nanowires in air at elevated temperature. The outward self-diffusion of metal-Asp precursors, the gas release of Asp oxidation, and the Kirkendall effect are essential for the formation of porous and tubular structures in the metal oxides. By choosing suitable metal-organic coordination nanowires as precursors, the facile strategy can efficiently synthesize porous nanotubes of other TMOs including NiO , NiCo_2O_4 , and Mn_3O_8 . Additionally, porous TMCs nanotubes (e.g. CoS_2 and CoSe_2) can also be acquired by the sulfuration or selenylation of metal-Asp nanowires in solution, further confirming the generality of our proposed metal-Asp self-template method in fabricating porous nanotubes of TMOs and TMCs with well open-ended channels and mesoporous walls. Taking Co_3O_4 as an example, the as-synthesized hierarchical porous nanotubes are found to be highly active materials for both electrocatalytic OER and anode in Li-ion battery.

Exploiting the coordination characteristics of transition-metal ions,^[14] metal-ion-based nanowires coordinating with L-aspartic acid (Metal-Asp) were fabricated as precursors. Using cobalt, the Co-Asp nanowires characterized by smooth

[*] H. Wang,^[‡] S. Zhuo,^[‡] Y. Liang, X. Han, Prof. B. Zhang
Department of Chemistry, School of Science, and Tianjin Key
Laboratory of Molecular Optoelectronic Science, Tianjin University
Tianjin 300072 (China)
E-mail: bzhang@tju.edu.cn

Y. Liang, X. Han, Prof. B. Zhang
Collaborative Innovation Center of Chemical Science and Engineer-
ing, Tianjin 300072 (China)

[‡] These authors contributed equally to this work.

Supporting information for this article can be found under:
<http://dx.doi.org/10.1002/anie.201603197>.

surfaces, average diameters of around 400 nm, and length up to several millimeters are successfully synthesized, as shown in the scanning electron microscopy (SEM) images (Figure 1a and Figure S1a,b in the Supporting Information). Transmission electron microscopy (TEM) image further reveals the solid nature of these nanowires (Figure S1c). In addition, scanning transmission electron microscopy energy dispersive spectroscopy (STEM-EDS) elemental mapping and Fourier transform infrared spectroscopy (FTIR) are utilized to illustrate the structure of these ultralong nanowires. As a result, the uniform distribution of elemental Co, C, and N (Figure 1b) and the characteristic vibration peaks (Figure S1d) unambiguously confirm the coordination character of Co^{2+} with Asp. The molecular formula of the coordination nanowires is proposed to be $\text{Co}(\text{Asp}) \cdot x\text{H}_2\text{O}$ based on the thermogravimetric analysis (TGA; Figure S2) and element-content analysis data (Table S1). In addition, the high crystallinity of these coordination nanostructures is verified

by the X-ray diffraction (XRD) pattern (see Figure 2g), and the sharp peak located at 6.6° reveals the coordination character as well.^[15] All of the results demonstrate that we have successfully fabricated the solid Co-Asp coordination nanowires using Asp as a chelating agent.

The as-prepared Co-Asp coordination nanowires further act as sacrificial templates and metal sources for the subsequent synthesis of Co_3O_4 mesoporous nanotubes (MNTs) in air by precisely controlling the oxidation conditions. SEM images (Figure 1c) show the open tubular structure of the as-synthesized products. TEM images (Figure 1d,e) further manifest the tubular character and porous tube wall of the as-converted samples. The as-converted nanotubes become much shorter than that of the precursors and their open ends have jagged edges (Figure 1c,d,e), indicating that the open ends in the as-converted nanotubes can be ascribed to the fracture of the ultralong nanowire precursors. This open-ended phenomenon cannot be observed in the self-template chemical transformation of nanorod-like and spherical precursors,^[16] confirming the importance of ultralong precursors in producing nanotubes. Meanwhile, all the diffraction peaks of these nanostructures in the XRD pattern (Figure 1g) can be clearly indexed as cubic Co_3O_4 with high purity (JCPDS No. 74-2120). The lattice spacing of 0.243 nm corresponding to (311) planes of cubic Co_3O_4 also confirms the good crystallinity of the porous tube walls (Inset of Figure 1e). Moreover, the characteristic peaks in the X-ray photoelectron spectroscopy (XPS) spectra (Figure S4) match well with previous reports on pure Co_3O_4 .^[17] And the Raman spectrum (Figure S4d) also excludes the presence of residual carbon, suggesting the complete transformation of precursors into Co_3O_4 . Furthermore, the concave profiles of element Co and O in the EDS line-scan elemental distribution (Figure 1f) strongly illustrate the tubular structure with high diameter-wall ratios as well. Remarkably, these hierarchical nanotubes own an average pore size of approximately 5.5 nm (Figure 1h) and a surface area of around $87.8 \text{ m}^2 \text{ g}^{-1}$, further confirming the mesoporous character of the as-converted nanotubes. These results indicate that the hierarchical Co_3O_4 nanotubes with open-ended channels and fine mesoporous walls have been successfully fabricated by the oxidation of the Co-Asp superlong nanowires.

To understand the mechanism underlying the oxidation induced chemical transformation, SEM, TEM, XRD, and EDS line-scan elemental distribution are adopted to characterize the intermediates, which are collected at different stages. When the Co-Asp nanowires are oxidized in closed air atmosphere at a slow heating rate of $0.5^\circ\text{C min}^{-1}$, a thin oxidized layer is formed on the surface of the solid nanowire precursors at 200°C (Figure 2b,e). The associated XRD pattern demonstrates that the intermediates consist of Co-Asp and Co_3O_4 (Figure 2h), indicating that the thin shell on the starting precursors is Co_3O_4 . Such an as-formed thin Co_3O_4 shell with many vacancies can be considered to be an interface to allow the outward diffusion of inner Co-Asp. The concave profiles of Co, C, and N element in the EDS line-scan elemental distributions (Figure 2e and Figure S6) suggest the outward diffusion of Co-Asp in the core of nanowires during

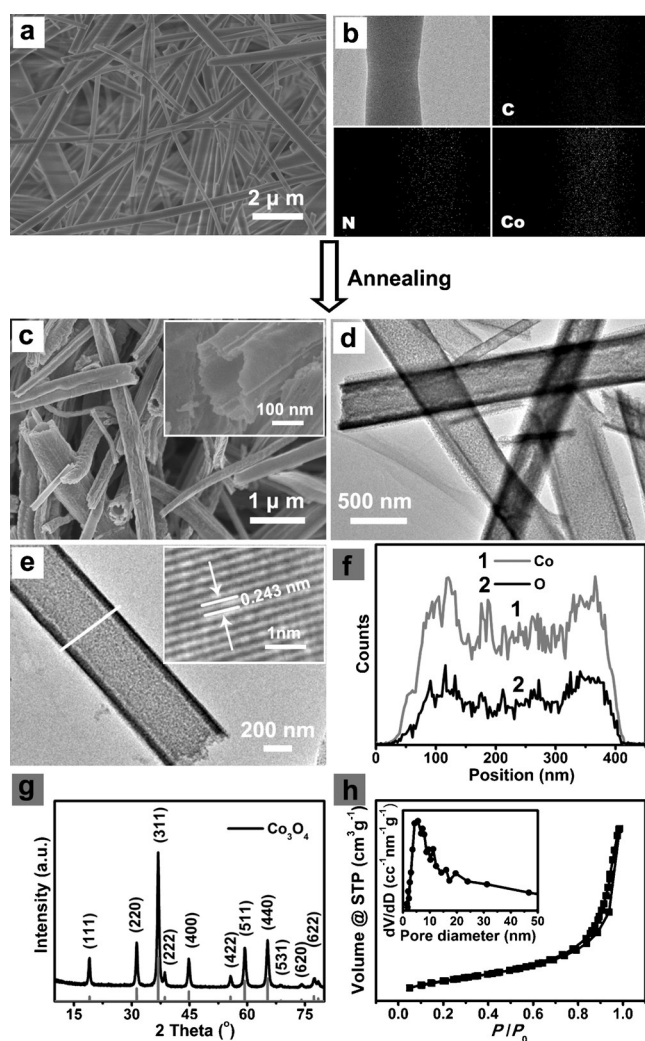


Figure 1. a) SEM image and b) STEM-EDS elemental mapping images of the solid Co-Asp superlong nanowires. c)–h) The as-converted Co_3O_4 mesoporous nanotubes: c) SEM image, d,e) TEM images, f) line-scan (along line in (e)) STEM-EDS elemental distributions, g) XRD pattern, and h) nitrogen adsorption/desorption isotherms. Inset: pore size distribution.

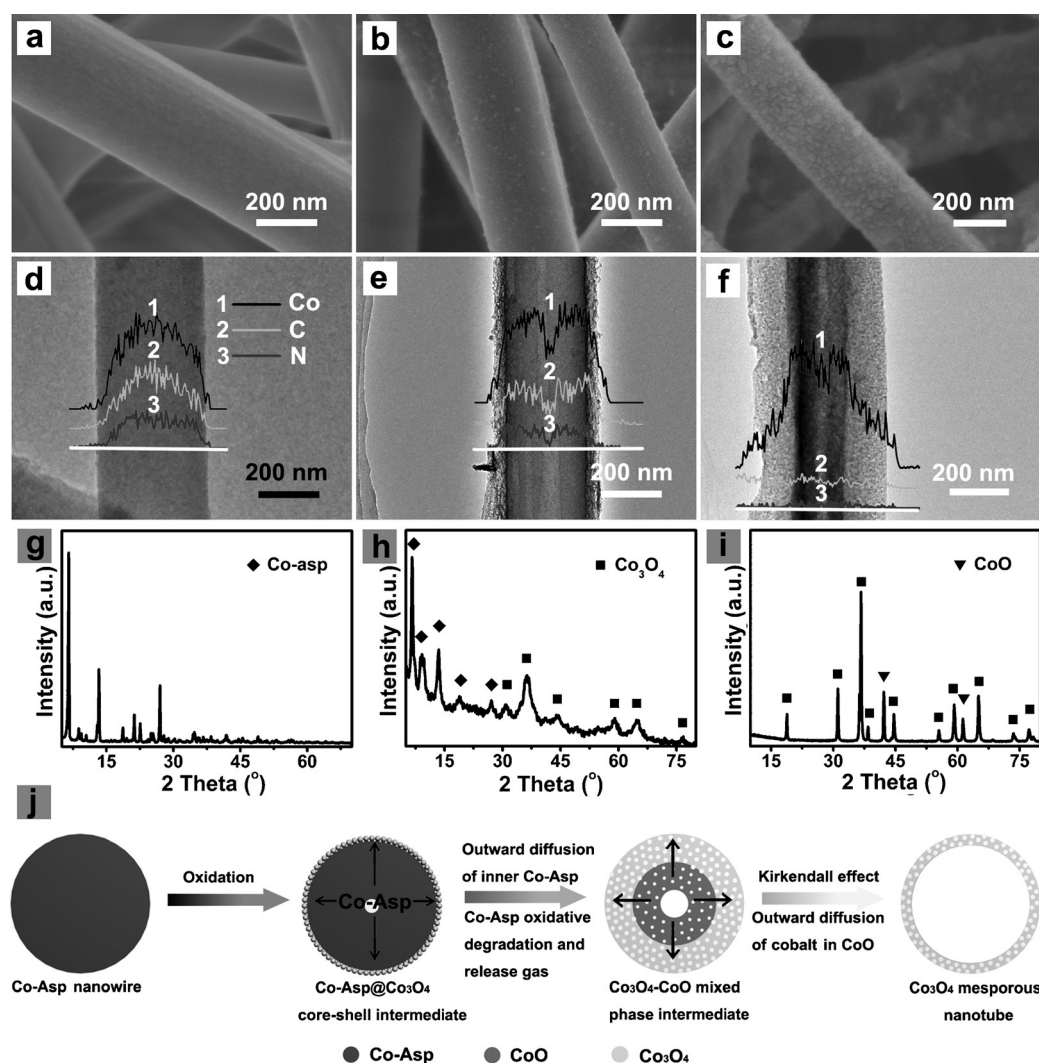


Figure 2. a)–c) SEM images, d)–f) TEM images, and line-scan STEM-EDS elemental distributions of Co, C, N and g)–i) XRD patterns of the intermediates collected at different reaction stages: 25 °C (a,d,g), 200 °C (b,e,h), 300 °C (c,f,i). j) Schematic illustration of the oxidation-induced, diffusion controlled synthesis of Co_3O_4 MNTs from the Co-Asp precursor nanowires.

the thermal oxidation process. The outward diffusion of Co-Asp should be induced by the oxygen in air, as observed in the outward motion of metal and carbon for metal atoms confined in a nanospace of carbon nanotubes.^[18] This conclusion is further supported by additional experiments performed in Ar or O_2 atmospheres (Figure S8). With the temperature gradually increased to 300 °C, the samples become hybrid Co_3O_4 -CoO porous architectures with a visible but unobvious tubular hollow region (Figure 2c,f). The appearance of nanopores can be mainly ascribed to the Asp-oxidation/degradation-derived gas release of the precursors. The formation of low-valence CoO may be due to the reducing gas from Asp thermal dissociation, as observed in WO_2 from thermal treatment of WO_3 -Amine precursors.^[19] Although there are some nanopores on the Co_3O_4 -CoO intermediates, the Co_3O_4 layer still blocks the direct oxidation reaction of inner Co^{2+} ions with the oxygen in air, to some extent. In the following transformation process, oxygen-

induced outward diffusion of cobalt ions,^[18] the merging of voids originated from the stain release caused by the lattice mismatch of CoO and Co_3O_4 , and the different diffusion rate of Co^{2+} and O^{2-} (Kirkendall effect) can make the tubular hollow region much bigger. Finally, the prolonged thermal oxidation at 300 °C can ultimately lead to the formation of mesoporous Co_3O_4 nanotubes with more obvious tubular structures (Figure 1c, d,e). Based on these experimental observations and discussions, a possible mechanism for the chemical conversion from solid Co-Asp nanowires into Co_3O_4 mesoporous nanotubes was proposed (Figure 2j). The transformation mechanism involves the initially formed Co_3O_4 layers, subsequent Co_3O_4 -CoO nanoporous tube-like intermediates, resulting from the combination of oxygen-induced outward diffusion of interior Co-Asp precursors and the gas release of

organic oxidation/dissociation, and resulting outward diffusion of Co^{2+} ions and the Kirkendall effect dominated formation of Co_3O_4 mesoporous nanotubes. Given the mechanistic insight into the transformation from Co-Asp nanowires to Co_3O_4 mesoporous nanotubes, the diffusion-dominated oxidation strategy should be suitable for synthesizing other TMOs mesoporous nanotubes. When Ni-Asp and NiCo_2 -Asp nanowires are adopted as the starting materials, the thermal oxidation strategy in air can produce mesoporous nanotubes of NiO and NiCo_2O_4 (Figure S10,11), respectively. Additionally, to rule out the effect of Asp, nitrilotriacetic acid (NA) is utilized to replace Asp as a chelating agent with metal ions to produce metal-coordinated precursors. As a result, the thermal oxidation of Mn-NA nanowires can lead to the formation of Mn_5O_8 mesoporous nanotubes (Figure S12), confirming the versatility of our proposed strategy in producing metal oxide nanotubes with well open-ended channels and mesoporous walls.

Furthermore, the Co–Asp nanowire precursors are found to be good candidates to the synthesis of CoS_2 and CoSe_2 mesoporous nanotubes (Figure S13,14) when the thermal oxidation process is replaced by the sulfuration or selenylation of metal–Asp nanowires in solution. These extending results confirm that our proposed self-template strategy of metal–organic coordination nanowires is a facile, efficient and highly versatile route to mesoporous nanotubes of transition metal oxides and chalcogenides.

The open-ended channels and mesoporous walls can endow the as-prepared hierarchical porous nanotubes with enhanced catalytic performance. Co_3O_4 mesoporous nanotubes (MNTs) are selected as typical examples to evaluate its applications towards electrocatalytic OER. The polarization curves (Figure 3a) show that the as-prepared Co_3O_4 MNTs

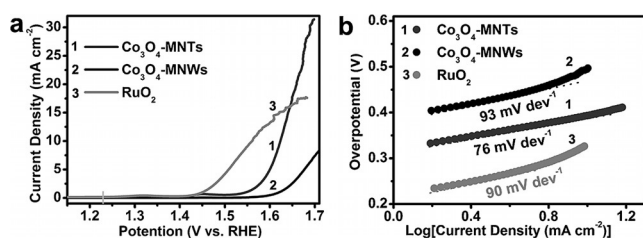


Figure 3. a) IR-corrected polarization curve and b) Tafel plots of porous Co_3O_4 nanotubes, porous Co_3O_4 nanowires, and commercial RuO_2 for water oxidation, loaded on glass carbon electrode in 0.1 M KOH solution at 5 mV s⁻¹.

supported on glassy carbon (loading mass: 0.208 mg cm⁻²) own a low onset potential of 1.54 V (vs. reversible hydrogen electrode (RHE)) and a required potential of 1.62 V (vs. RHE) for the current density of 10 mA cm⁻² in 0.1 M KOH aqueous solution, which are lower than those of the corresponding Co_3O_4 mesoporous nanowires (Figure S9, MNWs) and most of Co_3O_4 samples (Table S2). Notably, the OER current of the Co_3O_4 MNTs begin to exceed commercial RuO_2 particles when the applied potential surpass 1.645 V (vs. RHE) with a current density of about 16.1 mA cm⁻², despite the quite small onset potential of RuO_2 (1.42 V vs. RHE). And the Tafel slope of the MNTs (76 mV dec⁻¹) is much lower than those of MNWs (93 mV dec⁻¹) and commercial RuO_2 (90 mV dec⁻¹), indicating a more convenient charge transfer at the interface between Co_3O_4 MNTs and electrolyte (Figure 3b) because of the unique hierarchical mesoporous tubular architectures. Furthermore, promising practical application in OER is demonstrated with a much heavier load of Co_3O_4 MNTs on Ni foam (Figure S15).

The hierarchical mesoporous nanotubular structure can alleviate structural strain during the Li-ion charge–discharge process, and thus these Co_3O_4 MNTs are recognized as excellent anode materials for Li-ion battery (see Supporting Information). The significant potential of the Co_3O_4 MNTs as highly active and stable materials for Li-ion batteries and electrocatalytic OER are attributed to the improved permeation of electrolyte, much more active sites, and buffering volume and structural changes of porous nanotubes with mesoporous walls and open-ended tubes.

In summary, a generalized self-template strategy for the synthesis of transition-metal oxide (Co_3O_4 , NiO , NiCo_2O_4 , Mn_5O_8) hierarchical porous nanotubes has been successfully achieved via a facile oxidation-induced transformation at elevated temperature by using cheap and easy-prepared metal–organic coordination nanowires as sacrificial templates and metal sources. It is believed that the initial surface oxidation of the precursor, the subsequent outward diffusion of interior metal-coordinating components, the gas release from the oxidation/dissociation of the internal organic components, and the fracture of the ultralong precursors during the chemical transformation are vital to producing mesoporous nanotubes. Using Co_3O_4 as an example, the Co_3O_4 mesoporous nanotubes can not only display enhanced OER performance with a lower overpotential for the current density of over 16.1 mA cm⁻² compared with commercial RuO_2 , but also show optimal Li-ion battery capacity with high specific capacity, good cycling stability and excellent rate capability. Significantly, the oxidation process in air can be developed to sulfuration or selenylation in solution to obtain a series of metal chalcogenide porous nanotubes, such as CoS_2 , CoSe_2 , illustrating the universality of our methodology. In addition, considering the diversity of metal-coordination nanomaterials, our proposed generalized strategy may provide intriguing possibilities to develop many hierarchical, hollow, monocomponent, multicomponent, and heterogeneous nanostructures with enhanced performances in energy storage and catalysis.^[20]

Acknowledgements

This work was financially supported by the National Natural Science Foundation of China (No. 21422104).

Keywords: lithium-ion batteries · mesoporous nanotubes · oxygen evolution reaction · templates · transition metals

How to cite: *Angew. Chem. Int. Ed.* **2016**, 55, 9055–9059
Angew. Chem. **2016**, 128, 9201–9205

- [1] a) F. Caruso, R. A. Caruso, H. Möhwald, *Science* **1998**, 282, 1111; b) Y. Yin, R. M. Rioux, C. K. Erdonmez, S. Hughes, G. A. Somorjai, A. P. Alivisatos, *Science* **2004**, 304, 711; c) Y. Liu, J. Goebel, Y. Yin, *Chem. Soc. Rev.* **2013**, 42, 2610; d) J. Qi, X. Lai, J. Wang, H. Tang, H. Ren, Y. Yang, Q. Jin, L. Zhang, R. Yu, G. Ma, Z. Su, H. Zhao, D. Wang, *Chem. Soc. Rev.* **2015**, 44, 6749.
- [2] a) H. W. Liang, S. Liu, S. H. Yu, *Adv. Mater.* **2010**, 22, 3925; b) G. Zhang, B. Y. Xia, C. Xiao, L. Yu, X. Wang, Y. Xie, X. W. Lou, *Angew. Chem. Int. Ed.* **2013**, 52, 8643; *Angew. Chem.* **2013**, 125, 8805; c) B. Ni, H. Liu, P. Wang, J. He, X. Wang, *Nat. Commun.* **2015**, 6, 8756.
- [3] a) J. Liu, D. Xue, *Adv. Mater.* **2008**, 20, 2622; b) S. K. Han, C. Gu, M. Gong, S. H. Yu, *J. Am. Chem. Soc.* **2015**, 137, 5390.
- [4] a) W. Zhao, C. Zhang, F. Geng, S. Zhuo, B. Zhang, *ACS Nano* **2014**, 8, 10909; b) X. W. Lou, D. Deng, J. Y. Lee, J. Feng, L. A. Archer, *Adv. Mater.* **2008**, 20, 258.
- [5] S. Zhuo, Y. Xu, W. Zhao, J. Zhang, B. Zhang, *Angew. Chem. Int. Ed.* **2013**, 52, 8602; *Angew. Chem.* **2013**, 125, 8764.

- [6] a) T. Y. Ma, S. Dai, M. Jaroniec, S. Z. Qiao, *J. Am. Chem. Soc.* **2014**, *136*, 13925; b) H. B. Wu, B. Y. Xia, L. Yu, X. Y. Yu, X. W. Lou, *Nat. Commun.* **2015**, *6*, 6512.
- [7] a) H. Hu, B. Guan, B. Xia, X. W. Lou, *J. Am. Chem. Soc.* **2015**, *137*, 5590; b) G. Zhang, X. W. Lou, *Angew. Chem. Int. Ed.* **2014**, *53*, 9041; *Angew. Chem.* **2014**, *126*, 9187; c) S. Xu, C. M. Hessel, H. Ren, R. Yu, Q. Jin, M. Yang, H. Zhao, D. Wang, *Energy Environ. Sci.* **2014**, *7*, 632; d) J. Wang, N. Yang, H. Tang, Z. Dong, Q. Jin, M. Yang, D. Kisailus, H. Zhao, Z. Tang, D. Wang, *Angew. Chem. Int. Ed.* **2013**, *52*, 6417; *Angew. Chem.* **2013**, *125*, 6545.
- [8] a) C. Yuan, H. B. Wu, Y. Xie, X. W. Lou, *Angew. Chem. Int. Ed.* **2014**, *53*, 1488; *Angew. Chem.* **2014**, *126*, 1512; b) M. Chhowalla, Z. Liu, H. Zhang, *Chem. Soc. Rev.* **2015**, *44*, 2584; c) H. Wang, H. Yuan, S. S. Hong, Y. Li, Y. Cui, *Chem. Soc. Rev.* **2015**, *44*, 2664.
- [9] a) Y. Liang, Y. Li, H. Wang, J. Zhou, J. Wang, T. Regier, H. Dai, *Nat. Mater.* **2011**, *10*, 780; b) S. Gao, Y. Lin, X. Jiao, Y. Sun, Q. Luo, W. Zhang, D. Li, J. Yang, Y. Xie, *Nature* **2016**, *529*, 68.
- [10] a) C. Yan, G. Chen, X. Zhou, J. Sun, C. Lv, *Adv. Funct. Mater.* **2016**, *26*, 1428; b) Y. Dou, J. Xu, B. Ruan, Q. Liu, Y. Pan, Z. Sun, S. X. Dou, *Adv. Energy Mater.* **2016**, *6*, 1501835.
- [11] a) A. Bergmann, E. Martinez-Moreno, D. Teschner, P. Chernev, M. Gliech, J. F. Araujo, T. Reier, H. Dau, P. Strasser, *Nat. Commun.* **2015**, *6*, 8625; b) Y. Wang, T. Zhou, K. Jiang, P. Da, Z. Peng, J. Tang, B. Kong, W. B. Cai, Z. Yang, G. Zheng, *Adv. Energy Mater.* **2014**, *4*, 1400696.
- [12] a) Y. Sun, C. Liu, D. C. Grauer, J. Yano, J. R. Long, P. Yang, C. J. Chang, *J. Am. Chem. Soc.* **2013**, *135*, 17699; b) X. Yan, L. Tian, M. He, X. Chen, *Nano Lett.* **2015**, *15*, 6015.
- [13] G. Tong, J. Guan, Q. Zhang, *Adv. Funct. Mater.* **2013**, *23*, 2406.
- [14] H. Tong, Y. J. Zhu, L. X. Yang, L. Li, L. Zhang, *Angew. Chem. Int. Ed.* **2006**, *45*, 7739; *Angew. Chem.* **2006**, *118*, 7903.
- [15] L. Shen, L. Yu, H. B. Wu, X. Y. Yu, X. Zhang, X. W. Lou, *Nat. Commun.* **2015**, *6*, 6694.
- [16] L. Yu, L. Zhang, H. B. Wu, X. W. Lou, *Angew. Chem. Int. Ed.* **2014**, *53*, 3711; *Angew. Chem.* **2014**, *126*, 3785.
- [17] R. R. Salunkhe, J. Tang, Y. Kamachi, T. Nakato, J. H. Kim, Y. Yamauchi, *ACS Nano* **2015**, *9*, 6288.
- [18] J. Zhou, H. Song, X. Chen, J. Huo, *J. Am. Chem. Soc.* **2010**, *132*, 11402.
- [19] R. Wu, J. Zhang, Y. Shi, D. Li, B. Zhang, *J. Am. Chem. Soc.* **2015**, *137*, 6983.
- [20] a) Y. Zhao, X. Li, B. Yan, D. Xiong, D. Li, S. Lawes, X. Sun, *Adv. Energy Mater.* **2016**, 1502175; b) H. J. Lee, J. H. Lee, S. Y. Chung, J. W. Choi, *Angew. Chem. Int. Ed.* **2016**, *55*, 3958; *Angew. Chem.* **2016**, *128*, 4026; c) K. Li, J. Zhang, R. Wu, Y. Yu, B. Zhang, *Adv. Sci.* **2016**, DOI: 10.1002/advs.201500426.

Received: April 1, 2016

Published online: May 30, 2016